Physics Letters A 377 (2013) 932–939

Contents lists available at SciVerse ScienceDirect

Physics Letters A

www.elsevier.com/locate/pla

Shallow water rogue wavetrains in nonlinear optical fibers

Stefan Wabnitz [a,*], Christophe Finot [b], Julien Fatome [b], Guy Millot [b]

[a] Dipartimento di Ingegneria dell'Informazione, Università degli Studi di Brescia, via Branze 38, 25123, Brescia, Italy
[b] Laboratoire Interdisciplinaire Carnot de Bourgogne, UMR 6303 CNRS, Université de Bourgogne, 9 av. Alain Savary, 21078 Dijon, France

ARTICLE INFO

Article history:
Received 21 December 2012
Accepted 6 February 2013
Available online 8 February 2013
Communicated by V.M. Agranovich

Keywords:
Rogue waves
Nonlinear optics
Optical fibers
Phase modulation
Fluid mechanics

ABSTRACT

In addition to deep-water rogue waves which develop from the modulation instability of an optical CW, wave propagation in optical fibers may also produce shallow water rogue waves. These extreme wave events are generated in the modulationally stable normal dispersion regime. A suitable phase or frequency modulation of a CW laser leads to chirp-free and flat-top pulses or flaticons which exhibit a stable self-similar evolution. Upon collision, flaticons at different carrier frequencies, which may also occur in wavelength division multiplexed transmission systems, merge into a single, high-intensity, temporally and spatially localized rogue pulse.

1. Introduction

The dynamics of extreme waves, often known as freak or rogue waves, is presently a subject of intensive research in several fields of application [1,2]. In oceanography, rogue waves are mostly known as a sudden deep-water event which is responsible for ship wreakages. A relatively less explored, but potentially even more damaging manifestation of rogue waves also occurs in shallow waters, consider for example the propagation of tsunamis. In such environment, the crossing of waters propagating in different directions may lead to the formation of high-elevation and steep humps of water that result in severe coastal damages [3]. A universal model for describing the formation of deep-water rogue waves is provided by the one-dimensional Nonlinear Schrödinger Equation (NLSE). In this framework, rogue waves are linked with the presence of modulation instability (MI) [4], whose nonlinear development is described by the so-called Akhmediev breathers [5], and may ultimately result in the formation of the Peregrine soliton, a wave of finite extension in both the evolution and the transverse coordinates [6].

An ideal testbed for the experimental study of rogue waves is provided by optical pulse propagation in nonlinear optical fibers, which is closely described by the NLSE. Indeed, the statistics of spectral broadening in optical supercontinuum generation has been associated with extreme solitary wave emissions [7]. Moreover, the first experimental observation of the Peregrine solitons in any physical medium has been carried out exploiting the induced MI occurring in a highly nonlinear fiber [8].

In this Letter, we show that rogue waves in optical fibers may also be generated in the normal group-velocity dispersion (GVD) regime of pulse propagation, where MI is absent. Indeed, nonlinearity driven pulse shaping in this case may be described in terms of the semi-classical approximation to the NLSE [9], which leads to the so-called nonlinear shallow water equation (NSWE) [10], which is also known in hydraulics as the Saint-Venant equation [11]. Therefore we establish a direct link between the dynamics of extreme wave generation in shallow waters [12] and their direct counterparts in optical communication systems. Since the CW state of the field is stable, shallow water optical rogue waves may only be generated as a result of particular setting of the initial or boundary conditions. Namely, as discussed by Kodama and Biondini [13,14], the initial modulation of the optical frequency, which is analogous to considering the collision between oppositely directed currents near the beach, or the merging of different avalanches falling from a mountain valley.

In Section 2 we shall describe the dynamics of the generation of an intense, flat-top, self-similar and chirp-free pulse as a result of the initial step-wise frequency modulation of a CW laser. In hydrodynamics, this corresponds to the hump of water which is generated by two water waves traveling with opposite velocities. The intriguing property of such pulses, that we name flaticons, is their stable merging upon mutual collision into either a steady or transient high-intensity wave, as discussed in Section 3. The pulse collision dynamics may also lead to the formation of extreme intensity peaks in optical communication systems whenever various wavelength channels are transported on the same fiber. As pointed

* Corresponding author.
E-mail address: stefano.wabnitz@ing.unibs.it (S. Wabnitz).

0375-9601/$ – see front matter
http://dx.doi.org/10.1016/j.physleta.2013.02.007

out in Section 4, an interesting application of optical shallow water rogue waves is the possibility of generating, from a frequency or phase modulated CW laser, high repetition rate pulse trains with low duty ratio. In contrast with existing linear techniques for pulse train generation [15,16], rogue wavetrains lead to chirp-free, high-intensity pulse trains, which are important advantages for their possible use as communication signals.

2. Optical pulse dynamics

The propagation of pulses in optical fibers is described by the NLSE

$$i\frac{\partial Q}{\partial z} - \frac{\beta_2}{2}\frac{\partial^2 Q}{\partial t^2} + \gamma |Q|^2 Q = 0. \tag{1}$$

Here z and t denote the distance and retarded time (in the frame traveling at the group-velocity) coordinates; β_2 and γ are the group-velocity dispersion and the nonlinear coefficient, and Q is the field envelope. In dimensionless units, and in the normal dispersion regime (i.e., $\beta_2 > 0$), Eq. (1) reads as

$$i\frac{\partial q}{\partial Z} - \frac{\beta^2}{2}\frac{\partial q}{\partial T^2} + |q|^2 q = 0, \tag{2}$$

where $T = t/t_0$, $Z = z\gamma P_0 = z/L_{NL}$, $\beta^2 = \beta_2/(T_0^2 \gamma P_0) \equiv L_{NL}/L_D$, where L_{NL} and L_D are the nonlinear and dispersion lengths, respectively, $q = Q/\sqrt{P_0}$, t_0 and P_0 are arbitrary time and power units. Eq. (2) can be expressed in terms of the real variables ρ and u which denote the field dimensionless power and instantaneous frequency (or chirp)

$$q(T, Z) = \sqrt{\rho(T, Z)} \exp\left[-\frac{i}{\beta}\int_{-\infty}^{T} u(T', Z)\, dT'\right]. \tag{3}$$

By ignoring higher order time derivatives in the resulting equations (which is justified for small values of β), one obtains from the NLSE the semi-classical or hydrodynamic NSWE [9,10]

$$\frac{\partial}{\partial Z'}\begin{pmatrix}\rho \\ u\end{pmatrix} + \begin{pmatrix} u & \rho \\ 1 & u\end{pmatrix}\frac{\partial}{\partial T}\begin{pmatrix}\rho \\ u\end{pmatrix} = 0, \tag{4}$$

where $Z' = \beta Z$. In hydrodynamics, Eq. (4) describes the motion of a surface wave in shallow water, i.e., a wave whose wavelength is much larger than the water depth. In this context, ρ and u represent the water depth and its velocity, respectively. For a temporally localized input optical waveform such as a chirp-free square pulse (which is representative of the nonreturn-to-zero (NRZ) optical modulation format), i.e., with $\rho(T, Z = 0) = \rho_0$ for $|T| \leqslant T_0$ and $\rho(T, Z = 0) = 0$ otherwise, Eq. (4) may be analytically solved up to the point $Z' = T_0/\sqrt{\rho_0}$ in terms of the well-known Ritter dam-break solution [9,17]. Note that, at this point, the initial square NRZ pulse has broadened into a triangular pulse. In order to counteract such pulse deformation, it was proposed in [18] to use an input step-wise periodic frequency modulation, so that the self-phase modulation-induced chirp can be largely compensated for.

We are interested here in studying the behavior of the solutions of Eq. (4) with a dual quasi-CW pump input, that is we set $\rho(T, Z = 0) = \rho_0$, $\forall T$, and a periodic (with period T_M) frequency modulation, namely

$$u(T, Z = 0) = \begin{cases} u_0 & \text{for } -T_M/2 < T < 0, \\ -u_0 & \text{for } 0 < T < T_M/2, \end{cases} \tag{5}$$

so that in each modulation period there are two opposite frequency jumps. Indeed Eq. (5) corresponds to the injection of two

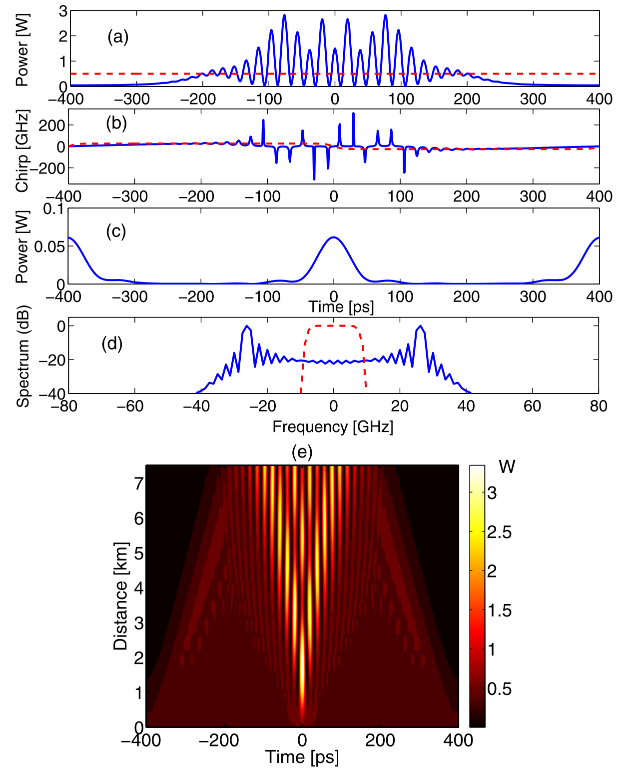

Fig. 1. Output (blue solid curves) and input (red dashed curves) power (a) and chirp (b) profiles from a 7 km long DCF in the linear case (i.e., with $\gamma = 0$); (c) output pulse power after a bandpass filter with 15.5 GHz bandwidth; (d) input and output spectral intensity (solid blue curve) and intensity transmission function of bandpass filter (dashed red curve); (e) contour plot of power profile vs. length.

time alternating, quasi-CW pumps at opposite frequencies $\pm u_0$, respectively (see the power spectrum in panel (d) of Fig. 1). Supposing that $u_0 > 0$, the frequency jump at $T = 0$ is such that, because of normal dispersion, the leading wave components at $T < 0$ travel slower than the trailing components at $T > 0$. Hence a wave compression (optical piston effect) at $T = 0$ results, which leads to a dispersive shock or optical wave-breaking. That is, high-frequency oscillations appear with a characteristic oscillation frequency equal to $1/\beta$. The opposite situation occurs for the frequency jump at $T = \pm T_M/2$, where dispersion leads to wave rarefaction, so that a dark pulse or hole develops.

Indeed, as shown in panel (a) of Fig. 1, high-intensity oscillations also occur in a purely linear dispersive medium (i.e., whenever $\gamma = 0$ in Eq. (1)), owing to the beating among the different frequency components which are generated by the initial condition Eq. (5), and that travel at different speeds. Here we show the output power profile from a 7 km long dispersion-compensating fiber (DCF) with normal GVD $D = -100$ ps/(nm km) (or $\beta_2 = 127$ ps^2/km) under purely linear propagation conditions. In Fig. 1 we considered a 1.25 GHz rate of frequency modulation with ± 26 GHz amplitude, and the input CW power $P = 500$ mW (or 27 dBm).

Panel (b) of Fig. 1 shows that in the linear case the output wavetrain develops a strong chirp as it propagates. Clearly in the absence of nonlinearity the spectrum of panel (d) in Fig. 1 remains unchanged, with most of its energy concentrated at the two quasi-CW pump frequencies. Therefore if we place a relatively narrow bandpass filter centered at the carrier frequency $u = 0$, we only obtain a weak (i.e., with a peak power which remains two orders of magnitude lower than the peak of the oscillations in panel (a) of Fig. 1) periodic pulse train (see panel (c) of Fig. 1). We used here a filter with the supergaussian spectral amplitude transfer function